

$[P_2W_{18}O_{62}]^{6-}$ . Experiments were carried out on the mixture. At pH 3 the  $Ru^{III/II}$ ,  $Ru^{IV/III}$ , and  $Ru^{V/IV}$  reduction potentials are  $-0.11$ ,  $+0.62$ , and  $+0.77$  V, respectively.  $^{31}P$  NMR:  $-17.1$  ppm (4.4 Hz),  $-59.2$  ppm (240 Hz). Substitution reactions with DMSO paralleled those of  $PW_{11}Ru^{II}$  and yielded  $\alpha_2$ - $[P_2W_{17}O_{61}Ru^{II}(\text{dms})]^{8-}$ , for which  $E(Ru^{III/II}) = +0.20$  V.  $^{31}P$  NMR:  $-8.7$  ppm (7.4 Hz) and  $-13.5$  ppm (7.4 Hz).

**Acknowledgment.** This work has been supported by the Na-

tional Science Foundation (CHE 8910921) and ARCO Chemical Co. Dr. Frank Liotta (ARCO) has independently prepared  $[PW_{11}O_{39}Ru^{II}(\text{dms})]^{5-}$ , and we thank him for the W NMR spectrum of this complex. We also thank Professor Andreas Ludi for a preprint and helpful advice on the synthesis of  $[Ru(\text{H}_2\text{O})_6]^{2+}$  and Professor Ronny Neumann for preprints of his catalysis work, for samples of the tungstosilicate derivatives, and for ongoing collaboration. Figure 1 was generated by SCHAKAL 88B/V16 (copyright Egbert Keller, University of Freiburg).

## The Persistent Radical Effect: A Prototype Example of Extreme, $10^5$ to 1, Product Selectivity in a Free-Radical Reaction Involving Persistent $\cdot\text{Co}^{II}$ [macrocycle] and Alkyl Free Radicals

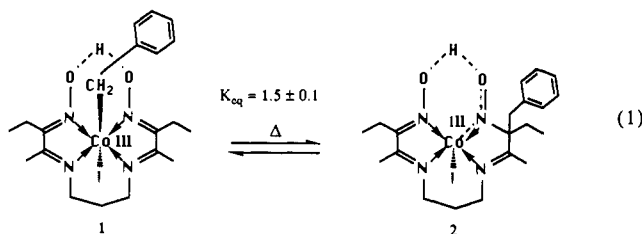
Brian E. Daikh and Richard G. Finke\*

Contribution from the Department of Chemistry, University of Oregon, Eugene, Oregon 97403. Received August 26, 1991

**Abstract:** Thermolysis of the coenzyme  $B_{12}$  model complex, **1**, leads to an equilibrium between **1** and the benzyl migration product **2**, but *not* to even a few percent of the usual radical-recombination product bibenzyl, eq 1. Further investigation of this intermolecular reaction between freely diffusing radicals has revealed a selectivity of ca.  $10^5$  to **1** (i.e., 99.999%) for **1** and **2** in comparison to bibenzyl (0.001%). General precedent for this result is found in a seminal paper by Fischer which outlines the criteria for such selectivity, but the present specific example provides a prototypical system for which the actual selectivity factor has been experimentally determined and which has been studied in detail. Numerical integration kinetic modeling of the formation of **2** from **1** over day time periods accurately predicts the formation of trace amounts of bibenzyl, consistent with our experimental results, while modeling over short times ( $\leq 100$  ms) confirms the major criteria for free-radical selectivity discussed by Fischer. Kinetic modeling over very long times (1000 years) provides the most dramatic illustration to date of Fischer's principle of "internal suppression of fast reactions" (the "persistent radical effect") by showing that only 0.18% of bibenzyl is formed even after a hypothetical 1000 years.

### Introduction

Recently we reported the unprecedented benzyl cobalt-to-carbon alkyl migration reaction shown in eq 1.<sup>1-3</sup> A detailed mechanistic study of this reaction<sup>1b</sup> indicated that this apparently intramolecular reaction in fact proceeds completely intermolecularly via the free-radical intermediates,  $\text{PhCH}_2\cdot$  and the stable ("persistent"), freely diffusing  $\cdot\text{Co}^{II}$ [macrocycle] radical. Excellent evidence for the mechanistic pathway in Scheme I was obtained.<sup>4</sup>



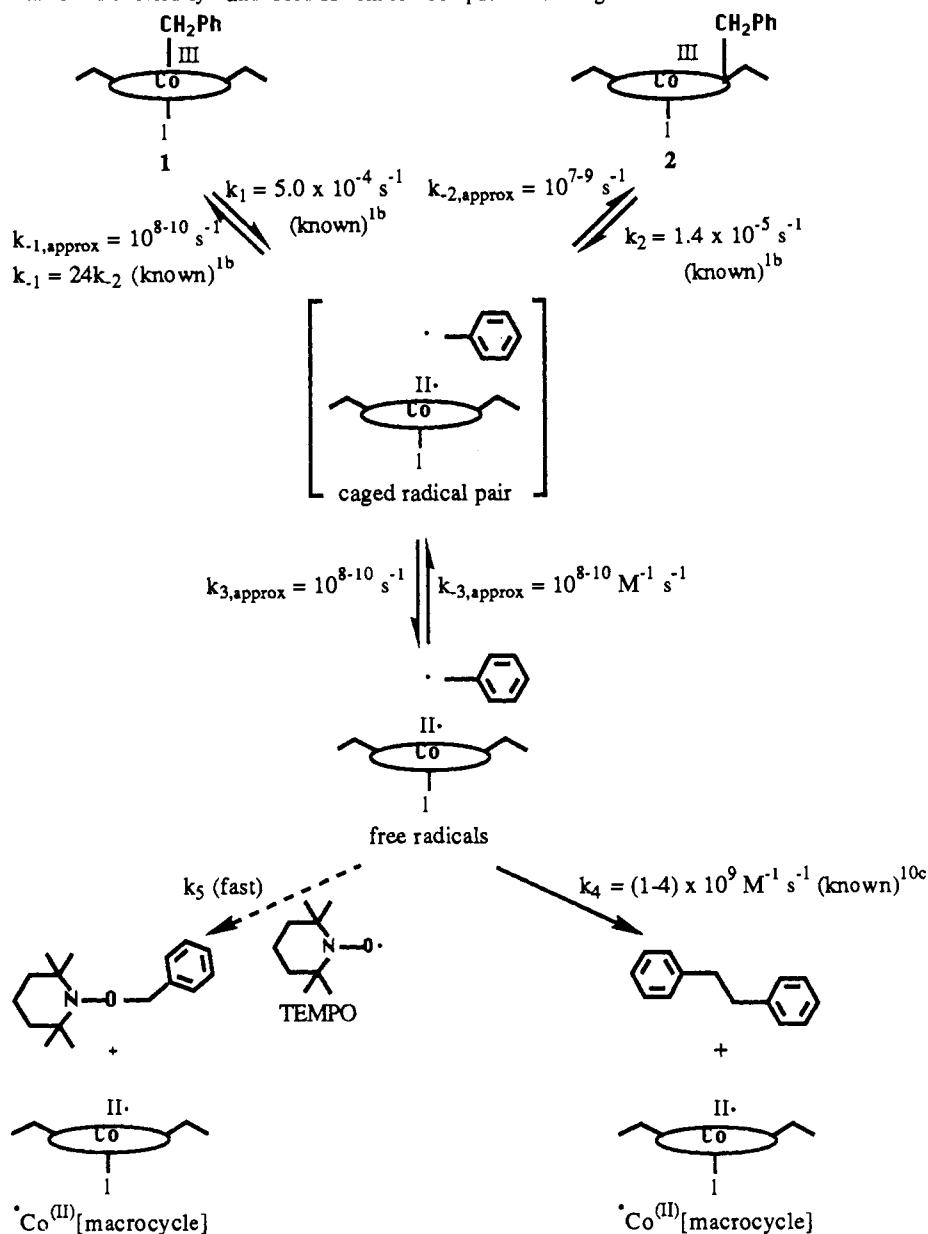
- (1) (a) Daikh, B. E.; Hutchison, J. E.; Gray, N. E.; Smith, B. L.; Weakley, T. J. R.; Finke, R. G. *J. Am. Chem. Soc.* **1990**, *112*, 7830. (b) Daikh, B. E.; Finke, R. G. *J. Am. Chem. Soc.* **1991**, *113*, 4160. (c) Daikh, B. E. University of Oregon Honors College Undergraduate Thesis, Eugene, OR, May 9, 1990.  
 (2) A study of the low, ca. 25 kcal/mol C-benzyl bond dissociation energy in **2**: Daikh, B. E.; Finke, R. G. *J. Chem. Soc., Chem. Commun.* **1991**, 784.  
 (3) An X-ray crystallographic investigation of the bonding changes accompanying the rearrangement of **1** to **2**: Daikh, B. E.; Weakley, T. J. R.; Finke, R. G. *Inorg. Chem.* **1992**, *31*, 137.

One of the few features of Scheme I that was not well understood before<sup>1b</sup> is the expected (but previously unverified and unquantitated) presence of bibenzyl. In fact, our earlier search for bibenzyl by NMR under conditions where 5% or more would have been detected proved negative;<sup>1</sup> this lack of the "expected" bibenzyl product was one of the initial reasons we chose to pursue this research.<sup>4b</sup>

In 1986, a seminal paper by Fischer appeared which included insightful suggestions by Ingold.<sup>5a</sup> This paper discussed, in a general way, how such free-radical reactions could be highly selective if two criteria were fulfilled:<sup>5</sup> (1) of the radical intermediates formed during the course of the reaction in question, one must be more persistent than the others, and (2) the persistent

- (4) (a) The mechanistic evidence includes (but is not limited to<sup>1b</sup>) a rate law starting with **1**, and with added free radical trap TEMPO (2,2,6,6-tetramethylpyridinyloxy free radical), that is inversely dependent on  $\cdot\text{Co}^{II}$ [macrocycle] and zero-order in added TEMPO<sup>4b</sup> (under conditions where the added TEMPO traps 100% of the benzyl radicals, i.e., where TEMPO appears in 100% of the products), demonstrating rate-determining Co-benzyl homolysis in **1**, and a rate law starting with **2** that is similarly zero-order in TEMPO under conditions where TEMPO appears in all the products, consistent with rate-determining C-benzyl homolysis in **2**.<sup>1b</sup> These and other data<sup>1b</sup> provide strong evidence for the mechanism shown in Scheme I. (b) Finke, R. G.; Smith, B. L.; Mayer, B. J.; Molinero, A. A. *Inorg. Chem.* **1983**, *22*, 3677.

- (5) (a) Fischer, H. *J. Am. Chem. Soc.* **1986**, *108*, 3925. (b) Selectivities of ca. 4:1 have been reported: Rügge, D.; Fischer, H. *Int. J. Chem. Kinet.* **1989**, *21*, 703.

Scheme I. Mechanism Established Previously<sup>1b</sup> and Used Herein for Computer Modeling<sup>a</sup>

<sup>a</sup>Known ca. 25 °C rate constants are labeled as such; rate constants labeled  $k_{x, \text{approx}}$  (25 °C) are estimates based on the literature.<sup>10</sup> (The left-most, dotted-line pathway dominates if the nitroxide free-radical trap TEMPO<sup>•</sup> is deliberately added to the reaction.<sup>1b</sup>)

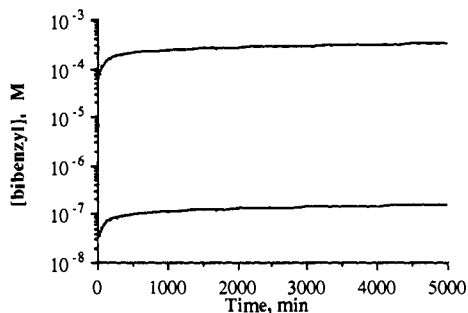


**Figure 1.** The range of possible bibenzyl concentrations over time as predicted by GEAR using the range of plausible values for the four unknown rate constants (i.e.,  $k_{-1}$ ,  $k_{-2}$ ,  $k_3$ , and  $k_{-3}$ ).<sup>10</sup> The lower curve will turn out to be the one consistent with the experimental results.

and transient species must be generated with equal rates. It is the initial buildup of the persistent intermediate which steers the reaction to follow a single pathway. Fischer called this the principle of "internal suppression of fast reactions";<sup>5</sup> an alternative and perhaps more descriptive phrase is the persistent radical effect.

However, no prototype, *highly selective* free-radical reaction<sup>5b</sup> illustrating the persistent radical effect has appeared where the exact level of selectivity (i.e., the ratio of **1** and **2** to bibenzyl in the present case) has been quantified and where the system has been studied, and is understood, in detail. It occurred to us that the rearrangement of **1** to **2** appeared to be providing just such a prototype reaction, depending upon the exact (unknown)<sup>1b</sup> yield of bibenzyl. Such highly selective free-radical reactions are a current topic of considerable interest in organic synthesis,<sup>6-9</sup> but

(6) Early lead references: (a) Tada, M.; Okabe, M. *Chem. Lett.* **1980**, 201. Okabe, M.; Tada, M. *Chem. Lett.* **1980**, 831. (b) Branchaud, B. P.; Meier, M. S.; Malekzadeh, M. N. *J. Org. Chem.* **1987**, *52*, 212 and references therein. (c) Bandaranayake, W. M.; Pattenden, G. *J. Chem. Soc., Chem. Commun.* **1988**, 1179 and earlier references in this series. (d) Ramakrishna Rao, D. N.; Symons, M. C. R. *J. Chem. Soc., Perkin Trans. II* **1983**, 187.

(7) (a) Branchaud, B. P.; Meier, M. S.; Malekzadeh, M. N. *J. Org. Chem.* **1987**, *52*, 212. (b) Branchaud, B. P.; Meier, M. S.; Choi, Y. *Tetrahedron Lett.* **1988**, *29*, 167. (c) Branchaud, B. P.; Meier, M. S. *Tetrahedron Lett.* **1988**, *29*, 3191. (d) Branchaud, B. P.; Choi, Y. L. *Tetrahedron Lett.* **1988**, *29*, 6037. (e) Branchaud, B. P.; Yu, G.-X. *Tetrahedron Lett.* **1988**, *29*, 6545. (f) Branchaud, B. P.; Choi, Y. L. *J. Org. Chem.* **1988**, *53*, 4638. (g) Branchaud, B. P.; Meier, M. S. *J. Org. Chem.* **1989**, *54*, 1320. (h) Branchaud, B. P.; Yu, G.-X. *Tetrahedron Lett.* **1991**, *32*, 3639.

the exact level of selectivity possible in free-radical reactions involving one or more persistent radicals has not been quantified and thus is not a generally appreciated point despite Fischer's seminal papers.<sup>5</sup>

Herein we report that the selectivity of **1** rearranging to **2** (or, equivalently, **2** rearranging to **1**) compared to the (low) yield of bibenzyl is an impressive and illustrative ca.  $10^5$  to 1. Also reported are quantitative kinetic modeling studies which allow detailed insights into the time course of all the reaction products and insights into how very high selectivities are accomplished in the reactions of reactive, freely diffusing radicals.

## Results and Discussion

**Initial Kinetic Modeling.** The kinetic modeling of the equilibrium reaction between **1** and **2** as well as the potential buildup of the  $^{\bullet}\text{Co}^{\text{III}}$ [macrocycle] and bibenzyl was performed prior to our experimental search for bibenzyl. This was done first because we wanted to *predict* the amount of bibenzyl (i.e., predict how difficult its detection was going to be). Then, assuming that any predicted concentration of bibenzyl was measurable, our goal was to experimentally demonstrate and quantitate its formation, thereby demonstrating consistency between the computer modeling and the experimental results.

The modified mechanistic scheme shown in Scheme I (i.e., without added nitroxide and thus where the only possible products are **1**, **2**,  $^{\bullet}\text{Co}^{\text{III}}$ [macrocycle], and bibenzyl) was computer modeled using the GEAR numerical integration program (see Scheme I and a footnote<sup>10</sup> for the rate constants employed). The results of the kinetic modeling over very short ( $\leq 100$  ms), medium (seconds to days), and very long (1000 years) reaction times are informative and will be discussed as is appropriate.

We initially modeled the buildup of  $^{\bullet}\text{Co}^{\text{III}}$ [macrocycle] and bibenzyl over the medium time range of 5000 min (3.5 days), the reaction time over which we performed our initial equilibrium (i.e.,  $\mathbf{1} \rightleftharpoons \mathbf{2}$ ) measurements.<sup>1b</sup> Because not all of the rate constants in Scheme I are known, the range of values found in Scheme I

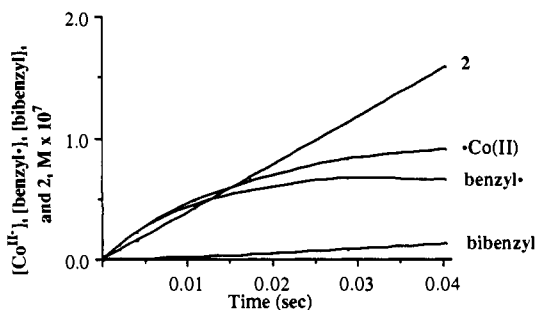


**Figure 2.** GEAR kinetic modeling of the time course of  $^{\bullet}\text{Co}^{\text{III}}$ [macrocycle], benzyl, bibenzyl, and **2** over extremely short reaction time (40 ms). The initial buildup of the persistent  $^{\bullet}\text{Co}^{\text{III}}$ [macrocycle] radical, relative to the recombination products **2** and bibenzyl, is consistent with Fischer's hypotheses as discussed in the text.

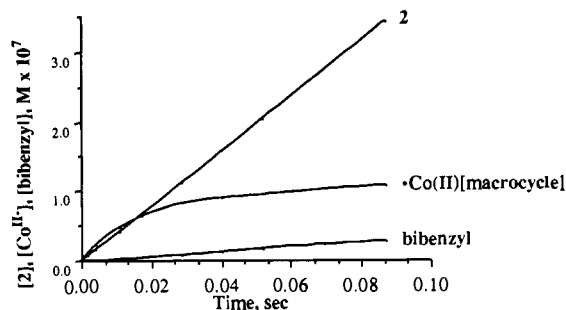


**Figure 3.** GEAR kinetic modeling of the time course of  $^{\bullet}\text{Co}^{\text{III}}$ [macrocycle], **2**, and bibenzyl over short reaction time (100 ms). Note that initially  $^{\bullet}\text{Co}^{\text{III}}$ [macrocycle] builds up to a higher level than **2** and bibenzyl but then quickly levels off while the concentration of **2** continues to increase. Note the high degree of selectivity (ca. 10:1) for **2** over bibenzyl even at this short reaction time.

(8) For lead references to more recent radical-alkene reactions via cobalt radical chemistry, see: (a) Bhandal, H.; Patel, V. F.; Pattenden, G.; Russell, J. J. *J. Chem. Soc., Perkin Trans. 1* **1990**, 2691. Patel, V. F.; Pattenden, G. *J. Chem. Soc., Perkin Trans. 1* **1990**, 2703. Bhandal, H.; Howell, A. R.; Patel, V. F.; Pattenden, G. *J. Chem. Soc., Perkin Trans. 1* **1990**, 2709. Coveney, D. J.; Patel, V. F.; Pattenden, G.; Thompson, D. M. *J. Chem. Soc., Perkin Trans. 1* **1990**, 2721, and earlier work in this series. (b) Ghosez, A.; Göbel, T.; Giese, B. *Chem. Ber.* **1988**, *121*, 1807. (c) Baldwin, J. E.; Li, C.-S. *J. Chem. Soc., Chem. Commun.* **1987**, 166. Baldwin, J. E.; Li, C.-S. *J. Chem. Soc., Chem. Commun.* **1988**, 261. Baldwin, J. E.; Moloney, M. G.; Parsons, A. F. *Tetrahedron* **1990**, *46*, 7263. (d) Scheffold, R. In *Studies in Organic Chemistry 30, Recent Advances in Electroorganic Synthesis*; Torii, S., Ed.; Elsevier: New York, 1987; p 275. Busato, S.; Tinembart, O.; Zhang, Z.-D.; Scheffold, R. *Tetrahedron* **1990**, *46*, 3155. Scheffold, R.; Abrecht, S.; Orliński, R.; Ruf, H.-R.; Stamouli, P.; Tinembart, O.; Walder, L.; Weymuth, C. *Pure Appl. Chem.* **1987**, *59*, 363.

(9) Low concentrations of cobaloximes have been used as catalytic chain-transfer agents in alkene radical polymerizations: Burczyk, A. F.; O'Driscoll, K. F.; Rempel, G. L. *J. Polymer Sci.* **1984**, *22*, 3255.

(10) (a) Known rate constants:  $k_1 = 5.0 \times 10^{-4} \text{ s}^{-1}$  (ref 4b);  $k_2 = 1.4 \times 10^{-5} \text{ s}^{-1}$  (ref 1b);  $k_4 = 1-4 \times 10^9 \text{ M}^{-1} \text{ s}^{-1}$  (ref 9c). Rate constant ranges<sup>10b,d</sup> used for predicting the plausible ranges of product concentrations shown in Figure 1:  $k_{-1} = 2.4 \times 10^8-2.4 \times 10^{10} \text{ s}^{-1}$ ,  $k_{-2} = 1 \times 10^7-1 \times 10^9 \text{ s}^{-1}$ ,  $k_3 = 1 \times 10^8-1 \times 10^{10} \text{ s}^{-1}$ ,  $k_{-3} = 1 \times 10^9-1 \times 10^{10} \text{ M}^{-1} \text{ s}^{-1}$ , and  $k_4 = 1-4 \times 10^9 \text{ M}^{-1} \text{ s}^{-1}$ . For Figures 2-6, the following refined set of rate constants was used. This set was chosen from among at least 30 trials for its ability to accurately reproduce the observed bibenzyl, **1** and **2** concentrations, and  $K_{eq}$ . Note that this set of rate constants is not claimed to be a unique set, and the individual rate constants themselves are unlikely to be accurate to better than  $10^{\pm 1}$ . However, this set more than suffices for the purposes of this paper (see the Experimental Section for further discussion of these points):  $k_{-1} = 3.1 \times 10^{10} \text{ s}^{-1}$ ;  $k_{-2} = 1.3 \times 10^9 \text{ s}^{-1}$  (these include the added constraint that  $k_{-1} = 24k_{-2}$ );<sup>1b</sup>  $k_3 = 2 \times 10^9 \text{ s}^{-1}$  (ref 10b,d);  $k_{-3} = 1 \times 10^{10} \text{ M}^{-1} \text{ s}^{-1}$  (ref 10b,d). (b) Finke, R. G.; Hay, B. P. *Polyhedron* **1988**, *7*, 1469 and refs 10 and 23 therein. (c) Burkhart, R. D. *J. Am. Chem. Soc.* **1968**, *90*, 273. (d) Cage escape and recombination rate constants estimates are based primarily on the following: Koenig, T. In *Organic Free Radicals*; Pryor, W. A., Ed.; ACS Symposium Series 69; American Chemical Society: Washington, DC, 1978; Chapter 9, p 134, and references therein. Koenig, T.; Scott, T. W.; Franz, J. A. In *Bonding Energetics in Organometallic Compounds*; Marks, T. J., Ed.; ACS Symposium Series 428; American Chemical Society: Washington, DC, 1990; Chapter 8, p 113; see Table II therein. For a review of radical-cage effects in organotransition-metal chemistry, see: Koenig, T. W.; Hay, B. P.; Finke, R. G. *Polyhedron* **1988**, *7*, 1499.

was tested. Though a range of values for  $k_{-1}$  and  $k_{-2}$  were used, in all cases the ratio of these two rate constants was fixed by  $k_{-1} = 24k_{-2}$ , a rigorous constraint experimentally established previously.<sup>1b</sup> The range of bibenzyl concentrations over the 5000 min time period (corresponding to the range of possible rate constants) is  $1.5 \times 10^{-7}-3.2 \times 10^{-4} \text{ M}$  bibenzyl as shown in Figure 1; this corresponds to 0.0008-2% of the initial concentration of **1**. (For all modeling experiments  $[\mathbf{1}]_0 = 0.02 \text{ M}$ , and the final  $^{\bullet}\text{Co}^{\text{III}}$ [macrocycle] concentration is simply twice the bibenzyl concentration, by mass balance.) In a moment we will see that the experimental bibenzyl concentration falls at the lower limit of the predicted possible range of [bibenzyl] values.

**Bibenzyl Detection and Quantitation.** On the basis of the possible lower limit of ca. 0.0008% bibenzyl predicted by the numerical integration kinetic studies, we designed a GC method for bibenzyl detection that was sensitive to ca. one-tenth this level. A solution from the  $\mathbf{1} \rightleftharpoons \mathbf{2}$  equilibrium mixture (80-fold concentrated; see the Experimental Section) was injected onto a carbowax capillary GC column. Because not all of the  $\mathbf{1} \rightleftharpoons \mathbf{2}$  mixture could be removed via the workup procedure (it is sparingly soluble in hexanes), it was necessary to use mild GC conditions (e.g., injector port and column temperatures both at 95 °C) which successfully minimized (see the Experimental Section) the formation of bibenzyl from **1** or **2** on the injector port or column. Consequently, the retention time for bibenzyl (mp = 50-53 °C; bp = 284 °C) was >20 min, and the peak was broad. As a control, a GC-MS of authentic bibenzyl using identical GC conditions was done to prove that the peak eluting at 20 min is in fact bibenzyl and not an artifact of some type; the observed fragmentation pattern of this peak matched the mass spectrophotometer's library pattern for bibenzyl identically.

Under the above conditions, bibenzyl was detected in the concentrated reaction mixture and replicate injections gave [bibenzyl] =  $(2.4 \pm 0.5) \times 10^{-5} \text{ M}$  from the precise area vs concentration calibration curve established for authentic bibenzyl under identical conditions (Table I, Experimental Section). After correcting for the small amount of bibenzyl formed from de-

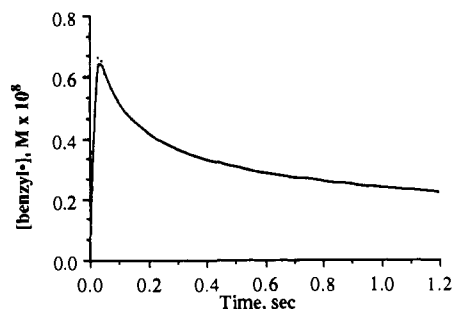


**Figure 4.** GEAR kinetic modeling of the time course of benzyl<sup>•</sup> radical over short reaction time (1.2 s). Note the initial buildup of the transient benzyl<sup>•</sup> radical in the first 50 ms, which thereafter quickly tapers away to reach a steady state concentration of ca.  $10^{-9}$  M.

composition ( $\leq 3\%$  of the observed bibenzyl), and after correcting for the 80-fold concentration factor introduced by our workup procedure, the [bibenzyl] formed in the thermolysis of **1** to give the **1**  $\rightleftharpoons$  **2** equilibrium mixture is  $(3.0 \pm 0.6) \times 10^{-7}$  M or just a mere 0.001% of the reaction products.

**Calculation of the Selectivity Factor.** The selectivity factor is simply the ratio of the total amount of **1** and **2** formed (or equivalently the initial amount of **1**, [1]<sub>i</sub>) to the amount of bibenzyl formed in the reaction mixture at any selected time: [1]<sub>i</sub>/[bibenzyl]. The actual value after 2 weeks reaction (>99.9% completion) is thus  $2.3 \times 10^{-2}$  M/ $3.0 \times 10^{-7}$  or  $8 \times 10^4$  before consideration of error estimates and then rounding off to  $10^5$ . In other words, the selectivity seen in this free-radical reaction<sup>11</sup> is an impressive  $10^5$  to 1, corresponding to a 99.999% selectivity.

**Additional Kinetic Modeling.** Additional kinetic modeling is desirable and is possible now that we know which rate constants to use (i.e., those that predict the correct [bibenzyl]).<sup>10</sup> The insights obtained from modeling over very short and very long times proved especially valuable.

The short time modeling verifies that an initial buildup of the persistent intermediate, <sup>•</sup>Co<sup>(II)</sup>[macrocycle], steers the reaction dramatically to form only specific radical recombination products. Figure 2 plots the time course of four species, <sup>•</sup>Co<sup>(II)</sup>[macrocycle], benzyl<sup>•</sup>, bibenzyl, and **2** over the first 40 ms of reaction time. It is clear from this plot that the <sup>•</sup>Co<sup>(II)</sup>[macrocycle] concentration initially builds up to a higher level than that of **2**. Figure 3 charts the concentration of <sup>•</sup>Co<sup>(II)</sup>[macrocycle], bibenzyl, and **2** for up to 100 ms of reaction. By this time the <sup>•</sup>Co<sup>(II)</sup>[macrocycle] and bibenzyl concentrations have begun to level off, while the concentration of **2** continues to build. Note that the high degree of selectivity for **2** compared to bibenzyl is already evident by this relatively short reaction time. From Figures 2 and 3 it is clear that the persistent intermediate, <sup>•</sup>Co<sup>(II)</sup>[macrocycle], initially builds up at a fast rate, consistent with Fischer's postulate, but then the rate slowly levels off, reaching essentially a steady-state level, and then increasing only *very slowly* over additional time.

Figures 2 and 4 monitor the interesting time course of the transient benzyl<sup>•</sup> radical. Figure 2 shows that in the first 10 ms, the benzyl<sup>•</sup> and <sup>•</sup>Co<sup>(II)</sup>[macrocycle] radicals are produced with equal rates (i.e., via homolysis of the Co–C bond in **1**) to yield equal concentrations. However, Figure 4 shows that the concentration of benzyl<sup>•</sup> peaks by the first 50 ms and by the first second has reached an almost steady-state concentration of ca.  $2 \times 10^{-9}$  M, about 2 orders of magnitude less than the concentration of the <sup>•</sup>Co<sup>(II)</sup>[macrocycle] persistent radical (which continues to increase). Figure 5 plots the time course of **1** and **2** over 5000 min (3.47 days), the time required for the reaction to go to 99.999% completion and in which **2** has reached its equilibrium concentration of 0.012 M, corresponding to a  $K_{eq} = 1.5$ . The solid

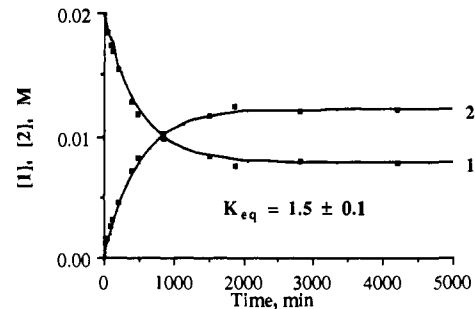


**Figure 5.** GEAR kinetic modeling of the concentration change of **1** and **2** over time. The solid lines represent modeled data using the rate constants found in ref 10, while the squares represent experimental data from **1**  $\rightleftharpoons$  **2** equilibrium measurements made previously.<sup>1</sup>

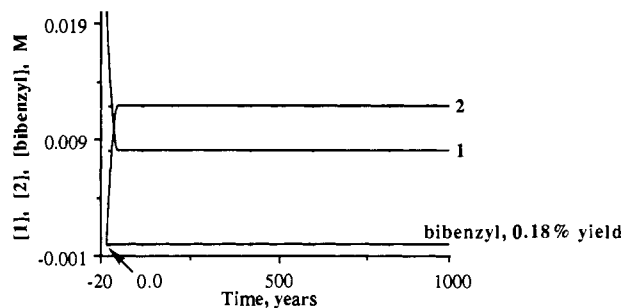


**Figure 6.** GEAR kinetic modeling of the time course of **1**, **2**, and bibenzyl over the extremely long, hypothetical reaction time of 1000 years. The yield of bibenzyl is ca. 0.18% due to the persistent radical effect (i.e., the product-steering effect of the buildup of the stable <sup>•</sup>Co<sup>(II)</sup>[macrocycle] radical that Fischer termed<sup>5</sup> "internal suppression of fast reactions").

lines represent the modeled data, while the squares are experimental data measured previously;<sup>1</sup> the excellent agreement between the calculated and experimental curves lends considerable support to our mechanistic scheme (Scheme I), to the refined set of rate constants<sup>10</sup> used for generating Figures 2–6, and to the numerical-integration kinetic-modeling methods employed herein.

Not shown in Figure 5 (since the concentrations are too low to be presented on the same graph) are the <sup>•</sup>Co<sup>(II)</sup>[macrocycle] and bibenzyl concentrations reached after 5000 min; the computed <sup>•</sup>Co<sup>(II)</sup>[macrocycle] concentration is ca.  $1 \times 10^{-6}$  M (0.005% of [1]<sub>initial</sub>), while the calculated bibenzyl concentration is ca.  $6 \times 10^{-7}$  (0.003% of [1]<sub>initial</sub>), the latter in reasonably good agreement with the experimental [bibenzyl] ( $3 \times 10^{-7}$  M). The important insight is that a concentration of only ca.  $1 \times 10^{-6}$  M of the persistent radical <sup>•</sup>Co<sup>(II)</sup>[macrocycle], corresponding to only 0.005% of the initial reactant **1** (or **2**), is enough to steer the reaction to a 99.999% product selectivity in the present case.

Another insight is that, in all of our numerical integration computations, the concentration of the caged-pair, PhCH<sub>2</sub><sup>•</sup>

<sup>•</sup>Co<sup>(II)</sup>[macrocycle], intermediate shown in Scheme I never exceeds more than ca.  $10^{-15}$  M. In other words, this intermediate could be omitted for all practical purposes if one so desires. However, we have retained its presence in Scheme I, in part because it is clear that radical-cage chemistry can no longer be neglected in organotransition-metal chemistry.<sup>10e</sup>

The fact that the concentration of bibenzyl after 5000 min is only  $10^{-6}$  M prompted us to ask the following: would a significant amount of bibenzyl be formed if the reaction were allowed to proceed for very long times.<sup>7</sup> In other words, *just how persistent is the persistent radical effect?* The kinetic modeling in Figure 6 shows that even after 1000 years, the concentration of bibenzyl still reaches only ca.  $3.5 \times 10^{-5}$  M or ca. 0.18% of the starting concentration of **1** (Figure 6). The persistent radical effect is indeed highly persistent! The internal suppression of the otherwise kinetically important recombination of two PhCH<sub>2</sub><sup>•</sup> radicals to yield bibenzyl operates essentially forever!

This result and the present system emphasize how an intermolecular equilibrium reaction involving only freely diffusing,

(11) Other factors contributing to the high selectivity are as follows: the lack of  $\beta$ -hydrogens in the alkyl (benzyl) ligand in the present case (and thus the impossibility of the otherwise common  $\beta$ -H elimination/disproportionation reaction); the choice of an aromatic solvent so that H<sup>•</sup> abstraction from the solvent by PhCH<sub>2</sub><sup>•</sup> is thermodynamically impossible; the use of rigorous O<sub>2</sub>-free techniques; and the use of mild temperatures where the <sup>•</sup>Co<sup>(II)</sup>[macrocycle] has prolonged stability.

reactive radicals can be extremely selective. Moreover, the selectivity and persistence of the selectivity should depend only on minimizing the other reaction channels available to the free radicals<sup>11</sup> (e.g., minimizing  $\beta$ -elimination<sup>9</sup> or H<sup>•</sup> abstraction from the solvent) and on maximizing the stability of the persistent radical involved<sup>9</sup> (including removing any adventitious reagents that will consume it, such as O<sub>2</sub> in the present case).

### Summary and Conclusions

The experimental and kinetic modeling results presented herein demonstrate that the rearrangement of **1** to **2** (or **2** to **1**) plus trace (0.001%) bibenzyl formation is an excellent example of how very high and long-lived selectivities can be achieved in reactions involving freely diffusing radicals. The key features necessary for the high selectivity in the present, perhaps best example to date, include those first noted by Ingold and Fischer<sup>5</sup> and verified herein by our short time kinetic modeling: (1) one of the radical intermediates formed during the course of the reaction must be more persistent than the others, and (2) the persistent and transient radicals (\*Co<sup>II</sup>[macrocycle] and benzyl\* in the present case) must be generated with equal rates. (They are in fact, i.e., via the homolysis of the Co-CH<sub>2</sub>Ph bond in **1** or the C-CH<sub>2</sub>Ph bond in **2**, respectively.) The initial buildup of the persistent intermediate then steers the reaction to follow a single pathway to **2** (and **1**), effectively excluding the formation of bibenzyl. Further insights as a result of the present study include the following: (3) the high level of selectivity possible, 10<sup>5</sup> to 1, (4) the experimental demonstration of this level of selectivity, (5) the importance of removing other reaction channels<sup>11</sup> to attain the highest selectivity, and (6) the insight that the selectivity of a reversible (equilibrium) reaction involving free radicals can persist essentially forever under the proper conditions.<sup>11</sup>

The present work also suggests that the rational design of highly selective reactions involving freely diffusing radicals should be a fertile area for future investigations. This seems likely given the availability of many absolute rate constants for free-radical reactions,<sup>12</sup> the ready availability of kinetic modeling, for example, via PC-based numerical-integration packages such as that used herein, the increasing number of persistent radicals, and thus the many unmodeled and experimentally untested possibilities for the development of new, highly selective free-radical reactions.<sup>13</sup>

### Experimental Section

**Reagents.** Benzene and hexanes (Baker Analyzed) were distilled under N<sub>2</sub> over Na and benzophenone and placed in the drybox where they were bubbled with box atmosphere for 1 h. Ethanol was distilled under reduced pressure from molecular sieves and stored in the drybox. Bibenzyl (Fisher Scientific) gave a satisfactory <sup>1</sup>H NMR spectrum and was used as received. Methylene chloride was bubbled with N<sub>2</sub> for 1 h and stored in the drybox.

**Equipment.** Air-sensitive reactions were done either in a nitrogen drybox (Vacuum Atmospheres, double length; O<sub>2</sub> levels averaged  $\leq$ 0.5 ppm) or in cuvettes sealed with Teflon screwcaps (Kontes). Light-sensitive alkyl-Co[macrocycle] compounds were protected from light by wrapping their containers in foil or electrician's tape. EPR spectra were recorded on a Bruker ESP 300 electron spin resonance spectrometer. Samples were prepared in the drybox in ethanol in quartz tubes fitted with air-tight caps. Analytical gas chromatography was done on a Hewlett Packard 5790A Series GC fitted with an Alltech Econo-cap carbowax capillary column, 30 m  $\times$  0.25 mm, i.d., film thickness = 0.25  $\mu$ m. Detection was by flame ionization. Mass spectra were recorded on a VG-12-250 mass spectrometer, 70-eV positive-ion mass spectrum. NMR spectra, referenced to the benzene protic impurity,  $\delta$  7.15, were recorded on a G.E. QE-300 spectrometer. Visible spectra were recorded on a Beckman DU-7 UV/visible spectrometer.

**Preparation of Compounds.** **1** and **2** were prepared by the methods previously reported<sup>1b,2</sup> and gave satisfactory elemental analyses and <sup>1</sup>H NMR and UV/visible spectra.

\*Co<sup>II</sup>[macrocycle]. This compound was also prepared by the method previously reported.<sup>4b</sup> In an inert atmosphere drybox 9.9 mg (0.028

mmol) of (OC)Co[C<sub>2</sub>(DO)(DOH)<sub>pn</sub>]I was dissolved in 100 mL of ethanol. To this solution was added 16.5 mg (0.0284 mmol) of Co<sup>III</sup>[C<sub>2</sub>(DO)(DOH)<sub>pn</sub>]I<sub>2</sub>, and the solution was stirred by magnetic stirrer until all solids were dissolved; the final solution was red. The ethanol was removed by vacuum rotoevaporation, and the brown solid was placed in a vial for storage. A small amount of residue was divided into three fractions, two dissolved in ethanol for visible and EPR spectroscopy analysis, and the third in benzene for visible spectroscopy analysis. One sample in ethanol and the sample in benzene were sealed in visible cuvettes fitted with Teflon screwcaps. These two samples were removed from the box and analyzed by visible spectroscopy. The sample in benzene gave the characteristic spectrum for \*Co<sup>II</sup>[C<sub>2</sub>(DO)(DOH)<sub>pn</sub>]I in that solvent,  $\lambda_{\text{max}} = 465$  nm. The sample in ethanol also gave the characteristic spectrum for that solvent,  $\lambda_{\text{max}} = 520$  nm. The room temperature EPR spectrum for 10<sup>-3</sup> M \*Co<sup>II</sup>[C<sub>2</sub>(DO)(DOH)<sub>pn</sub>]I in ethanol also matched the characteristic spectrum for this compound.<sup>14</sup> EPR parameters were as follows: microwave frequency, 9.79 GHz; microwave power, 25 mw; receiver gain, 5.3  $\times$  10<sup>3</sup>; modulation frequency, 50.0000 kHz; modulation amplitude, 10.000 G; conversion time, 5.12 ms; time constant, 0.64 ms; sweep time, 5.243 s; center field, 3000.00 G; sweep width, 1500.00 G.

**Kinetic Modeling.** Numerical integration of the modified mechanistic scheme (Scheme I, i.e., the **1**  $\rightleftharpoons$  **2** equilibrium reaction) was done using the GEAR integration package.<sup>15</sup> Using the PRGEAR portion of the program, a GEAR file was prepared from Scheme I. Known rate constants were used when possible (i.e.,  $k_1$ ,  $k_2$ , and  $k_4$ ). When exact rate constants were not available, reasonable approximations were made from literature estimates, and the experimentally established<sup>1b</sup> constraint that  $k_{-1} = 24 \cdot k_{-2}$  was placed on these unknown values. Scheme I was modeled over very short (i.e.,  $\leq$ 100 ms), medium (i.e., second-days), and very long (i.e., 1000 years) reaction times to monitor the time course of reaction products and intermediates. Initially (i.e., prior to the experimental determination of the actual [bibenzyl]), the full range of plausible values<sup>10</sup> for the unknown rate constants (i.e.,  $k_{-1}$ ,  $k_{-2}$ ,  $k_3$ , and  $k_{-3}$ ) was used in order to establish minimum and maximum concentration ranges for the species of interest, see Figure 1. Then, once the experimental [bibenzyl] was determined to be 0.001% of the [I]<sub>initial</sub>, a "best" set of rate constants consistent with this fact was discovered by trial and error ( $\geq$ 30 trials) and then used in all the subsequent kinetic modeling, Figures 2-6. This set of rate constants is  $k_1 = 5.0 \times 10^{-4} \text{ s}^{-1}$ ,  $k_{-1} = 3.1 \times 10^{10} \text{ s}^{-1}$ ,  $k_2 = 1.4 \times 10^{-5} \text{ s}^{-1}$ ,  $k_{-2} = 1.3 \times 10^9 \text{ s}^{-1}$ ,  $k_3 = 2 \times 10^9 \text{ s}^{-1}$ ,  $k_{-3} = 1 \times 10^{10} \text{ M}^{-1} \text{ s}^{-1}$ , and  $k_4 = 1 \times 10^9 \text{ M}^{-1} \text{ s}^{-1}$ . Note, however, that no claim for uniqueness (e.g., in terms of fitting the observed bibenzyl concentration) is made for this "best" set of rate constants thought to be no better than 10<sup>±1</sup> for any individual rate constant. This level of precision is quite acceptable, however, since the only crucial requirement is that the set used correctly describes the rates of formation of **1** and **2** and the yield of bibenzyl, which the employed set of rate constants in fact do.

In order to obtain accurate low concentration data from the kinetic modeling, it was necessary to change one of the integration parameters from its default value. Specifically, for the generation of the data used in all of the figures, the error test constant was changed to  $1.0 \times 10^{-9}$  (the minimum integration stepsize was maintained at the default value of  $1.0 \times 10^{-12}$ , and the maximum integration stepsize was also maintained at the default value of  $1.0 \times 10^3$ ).

**Thermolyses to Yield Bibenzyl (Plus **1** and **2**).** Numerous thermolysis experiments were done under identical experimental conditions, varying only the time of the thermolysis. A typical experiment is described below. (In what follows, the secondary Schlenk tube is used to further protect against oxygen leakage over long reaction times; the benzene in the secondary tube is used simply as a heat-transfer medium.) In the drybox 80.5 mg (0.148 mmol) of **1** was dissolved in 6.50 mL of benzene in the dark: [I] =  $2.28 \times 10^{-2} \text{ M}$ . Next, 4.50 mL of this solution was sealed in an airtight cuvette wrapped in foil and fitted with a Teflon screwcap. This cuvette was placed inside a Schlenk tube, and the tube was filled with benzene up to the bottom of the screwcap so that the cuvette was immersed. The outer Schlenk tube was then sealed with a ground glass stopper with grease. Tape was wrapped around the outer tube and stopper to prevent the top from popping off under higher pressures. The outer tube was wrapped in foil, removed from the drybox, and placed in a 69.0  $\pm$  0.2 °C oil bath for two weeks. The remaining 2.00 mL of solution were sealed in another foil-wrapped cuvette and treated by the same method.

**Post Thermolysis Workup of the Reaction Mixtures.** All reaction mixtures were treated by the same method; an example is described. After the solution of **1** had been thermolyzed for a designated amount

(12) For example: *Radical Reaction Rates in Liquids*; Fischer, H., Ed.; Springer: Berlin, 1983; Landolt-Bornstein, New Series, Group II, Vol. 13.

(13) For instance, one speculative and untested possibility for a new class of selective free-radical reactions might involve having more than one persistent radical present.

(14) Finke, R. G.; McKenna, W. P.; Schiraldi, D. A.; Smith, B. L.; Pierpont, C. *J. Am. Chem. Soc.* **1983**, *105*, 7592; see p 7603 and ref 54.

(15) Stabler, R. N.; Chesick, J. *Int. J. Chem. Kinet.* **1978**, *10*, 461.

Table I

wt of peak (mg)	[bibenzyl] in 80-fold pre-concentrated solution	[bibenzyl] in original reaction solution
7.3	$2.0 \times 10^{-5}$ M	$2.5 \times 10^{-7}$ M
11.4	$2.9 \times 10^{-5}$ M	$3.6 \times 10^{-7}$ M
9.0	$2.4 \times 10^{-5}$ M	$3.0 \times 10^{-7}$ M
	[bibenzyl] = $(2.4 \pm 0.5) \times 10^{-5}$ M	[bibenzyl] = $(3.0 \pm 0.6) \times 10^{-7}$ M

of time (at least enough to reach the 60% 2/40% 1 equilibrium mixture) the cuvette was removed from the oil bath and taken into the drybox. The cuvette, continuously foil-wrapped, was opened, and 0.5 mL of solution was removed. The benzene from this 0.5 mL sample was removed by vacuum rotoevaporation, and the residue was redissolved in a similar volume of benzene- $d_6$ , sealed in an airtight NMR tube, and analyzed by  $^1\text{H}$  NMR.

The remaining reaction mixture was worked up in the following manner. The benzene from a post-thermolysis mixture was removed by rotoevaporation; note that a knowledge of the number of millimoles (i.e., the original volume and concentration, 4.0 mL of  $2.3 \times 10^{-2}$  M) is required to calculate the 80-fold concentration factor determined below. The residue was triturated six times with 10-mL portions of hexanes (60 mL total) to extract any bibenzyl, leaving most, but not all of 1 and 2 behind. The hexanes were then removed by rotoevaporation, and the resulting residue was resuspended in a known volume of benzene (specifically 0.050 mL; a net 80-fold concentration factor resulted from this procedure). The sample, which was light orange in color (indicating slight contamination with 1 and 2), was then analyzed by GC and EPR.

**Bibenzyl Detection and Quantitation.** Optimal conditions for detecting bibenzyl, while minimizing the amount of bibenzyl formed from 1 or 2 on the injector port, were experimentally determined to be as follows: flow rate =  $0.003 \text{ mL}\cdot\text{min}^{-1}$ , injector =  $95^\circ\text{C}$ , column =  $95^\circ\text{C}$ , detector =  $225^\circ\text{C}$ , att. = -2, thresh = -2; retention volume = 0.06 mL (retention time = 21.5 min at a flow rate of  $0.003 \text{ mL}\cdot\text{min}^{-1}$ ). To determine that the peak at 21.5 min is in fact bibenzyl and not an artifact of the GC method, an authentic sample was analyzed by GC-MS under identical conditions. The corresponding peak by GC-MS had the identical fragmentation pattern as the mass spectrometer's library spectrum for authentic bibenzyl.

To determine the limit of detection and to generate a calibration curve for quantifying bibenzyl by GC, solutions of authentic bibenzyl in benzene from  $2.6 \times 10^{-3}$ – $2.6 \times 10^{-6}$  M were prepared and subjected to GC, and their respective peak weights were plotted versus concentration. (Because some peaks corresponding to low concentrations were detectable but not always integrated accurately by the GC integrator, all peaks were enlarged by Xerox, then cut, and weighed, and their respective weight plotted versus the corresponding concentration. Peaks corresponding to  $<1 \times 10^{-6}$  M were not detectable above the baseline.) The resulting highly linear and thus quite precise calibration curve is fit by the equation  $y = (4.59 \pm 0.01) \times 10^5 X - (2 \pm 3)$ ,  $R^2 = 0.99998$ , and was used for conversion of all subsequent bibenzyl GC peak weights to concentrations.

Aliquots (1–5  $\mu\text{L}$ ) of the worked up, 80-fold concentrated reaction mixture were injected onto the GC column. The areas of the corresponding bibenzyl peaks (as judged by both retention time and co-injection of authentic material) were then converted to concentrations via

the calibration curve, and then these concentrations were converted to initial reaction mixture concentrations by dividing by the 80-fold concentration factor. These results are tabulated in Table I.

Because the worked up solutions that were analyzed by GC were visibly colored by contamination of a small amount of 1 and 2, control experiments were needed to address the concern that part (or possibly even all) of the bibenzyl being observed was formed from decomposition of 1 and 2 on the injector port and not from the thermolysis reaction itself. Hence, as a control, solutions of authentic 1 in benzene approximating the concentration of 1 and 2 in the worked up reaction mixture ( $10^{-4}$ – $10^{-3}$  M by UV/visible spectroscopy) were injected and the amount of bibenzyl quantified. Of these solutions, the only one that gave a detectable bibenzyl peak was ca.  $10\times$  more concentrated in 1 ( $1.1 \times 10^{-3}$  M) than the 80-fold concentrated reaction solution. This peak corresponds to a weight of 0.9 mg which in turn corresponds to a concentration of  $6 \times 10^{-6}$  M bibenzyl. Taking into account that this solution of 1 is ca.  $10\times$  more concentrated than the 80-fold concentrated solution, the amount formed by decomposition in that solution is then ca.  $6 \times 10^{-7}$  M. This allows calculation of the difference between the mean concentration of bibenzyl in the 80-fold concentrated reaction mixture and the bibenzyl formed on the injector port,  $2.4 \times 10^{-5}$ – $6.0 \times 10^{-7}$  M or  $2.3 \times 10^{-5}$  M. That is, *at most*, only ca. 3% of the detected bibenzyl is formed by decomposition on the injector. The concentration of bibenzyl formed in the thermolysis reaction itself is then 1/80th this value or  $3.0 \times 10^{-7}$  M, 0.001% of the initial concentration of 1.

**Attempted  $^{60}\text{Co}(\text{II})$ [macrocycle] Detection.** The goal of these experiments was to see if we could monitor the trace production of  $^{60}\text{Co}(\text{II})$ [macrocycle] by EPR; the reaction mixture was analyzed by EPR both before and after workup in an attempt to detect this species. These experiments were unsuccessful, but control experiments established that the detectability limit (under our exact conditions and EPR instrument parameters) was ca.  $10^{-4}$  M, whereas the expected  $^{60}\text{Co}(\text{II})$ [macrocycle] concentration was  $10^3$  lower, ca.  $10^{-7}$  M. Further details are available as supplementary materials.

**Acknowledgment.** Support from NIH Grant DK 22614 is gratefully acknowledged. We also thank Professor Bruce Branchaud at Oregon for helpful discussions.

**Registry No.** 1, 87319-52-6; 2, 133470-79-8; bibenzyl, 103-29-7; coenzyme B<sub>12</sub>, 13870-90-1.

**Supplementary Material Available:** Experimental details for the attempted quantitation of  $^{60}\text{Co}(\text{II})$ [macrocycle] by EPR (2 pages). Ordering information is given on any current masthead page.